Journal of Engineering and Applied Sciences 11 (6): 1355-1362, 2016
ISSN: 1816-949X

Using the Force Decomposition Method to Study in the Thrust Mechanisms of Flexibility on Bionic Structure Motion

Jen-Yi Chang
Tainan University of Technology, Tainan, Taiwan

Abstract: It is difficult to identify the thrust due to the vortices generated by an undulating motion as well as the shape and frictional drag as fish swims forward and encounter. This is because that the direction of thrust and drag are opposite but in the same direction. In this study, we investigate the hydrodynamics of an undulating fish-like bionic structure model from the perspective of force decomposition and the associated force elements. Each bionic structure undergoes lateral motion in the form of a stream wise travelling wave. It's shown that added-mass force is the most significant thrust source among all considered motions and arrangements. By identifying the variations of the vorticity thrust elements with various flow structures, we found that the vortices round the leeside of deformable body are beneficial for thrust generation; however, the average volume vorticity contribution is opposite to swim forward. These results lead to understand why inviscid theory proposed by Lighthill and Wu could be used to explain propulsion of fish.

Key words: Force decomposition method, thrust mechanisms, bionic structure motion, variations, Taiwan

INTRODUCTION

The effects of body flexibility on aquatic and flight locomotion have been of interest to researcher. It has been shown that for flying insect the flexible-wing flapping can be more efficient in lift generation. Besides, a bending body or caudal of aquatic animal can increase both efficiency and thrust. Understanding the hydrodynamic characteristic for a deformable body moving around in flow is helpful to design and construct biomimetic propelled devices such as underwater and micro-aerial vehicles. In this study, we concern ourselves with the propulsive mechanisms of two types of motion: one is a fish-like undulation motion and the other is a heaving motion with flexibility by investigating various force contributions due to the added-mass effect, the vorticity in the flow as well as on the body surface.

Fish perform a large variety of swimming movements and most of them generate a propulsive force by passing a backward-progressing wave along the body. In general, swimming propulsive modes can be primarily classified into three categories based on the envelope shape of the body. The mode is called Anguilliform if large amplitude undulations exist along the whole body, Carangiform if the undulations are only in the posterior part of the body, and Thunniform if the oscillations are restricted only at the tail. Each swimming mode has its exclusive abilities; for instance, the Thunninform is known as the most efficient locomotion mode (Lighthill, 1970) and the Anguilliform swimmers can alter the propagation direction of the wave to control backward or forward swimming. More detail review on the fish swimming modes and characterizes can be found by Sfakiotakis *et al*. (1999).

The body moving in a small viscous flow generates a series of coherent vortices shedding behind the body. Observation of flexible motion such as swimming fish reveals different types of wakes behind them which apparently play an important role in the mechanisms of thrust production. A simple two-dimensional oscillating or undulating body under appropriate kinematical conditions can produce a series of thrust-type vortices, terms as a reversed Karman vortex street. These vortices comprise regions of vorticity in alternating sign and are aligned on either side of body's trajectory to produce a jet-like backward velocity in the wake, carrying fluid momentum. Based on the jet reaction principle, there is a net thrust exerted on a body. Also, a series of continuous and lined vortex rings are generated behind three dimensional periodic oscillating and undulating bodies. Although these wake structures are more complicated and diverse compared to that in two dimensions, the basic principles of explaining thrust generation would be the same.

Significant theories have been developed to calculate the thrust generated by prescribed motions of a rigid or deformable body in high-Reynolds-number incompressible flow (Lighthill 1986; Wu, 1981). In nature, the problems in fish swimming and insect flight are complicated because they involve fluid-body interactions. An instantaneous motion of the flexible body is

determined not only by the forces from the ambient fluid but also by embedded muscles with internal body elastic forces, forming a couple dynamical system. However, investigating the mechanism for the prescribed deformation of body is still important to understand the locomotion of many swimming and flying organisms (Alben, 2008). In the literature, there are several useful mathematical models which describe kinematics of fish swimming and shed light on different aspects of hydrodynamic force. A quasi-static approach (Taylor's resistive model) is based on steady-state flow theory to calculate the forces by means of sequential frames of fish motion. However, it is over simplified due to ignoring inertial force and is restricted to low Reynolds numbers flows. Lighthill is one of major contributors to develop mathematical theories to understand the physical insight of many aspects of fish locomotion (Lighthill, 1960, 1969, 1970). The elongated body theory (Lighthill, 1960) also called by reactive elongated body theory or slender body theory, assuming a frictionless fluid (high-Reynolds-number incompressible flow), considers that the acceleration reaction is the main propulsive force for undulating fish. It predicts well the thrust for the sub carangiform and carangiform modes. Later, lighthill extended the elongated body theory to be more suitable to the large lateral motion of the caudal fin for carangiform modes, called by large-amplitude elongated-body theory. Waving plate theory originally proposed by Wu (1981) is to treat the fish as an elastic waving plate swimming in an inviscid fluid. The oscillatory Foil theory (Wagner *et al.* 1925) which applies to analyze lift generation for an airfoil is applicable to study the thrust for the carangiform locomotion and the tuna oscillatory. Derived from the slender body theory, bulk momentum (or Bulk flow) theory (Blake, 1983) is most commonly used to investigate bio-fluid mechanisms for aquatic animals. It supposes that the total momentum of fluid given by all the body elements is equal to the momentum of fluid released from the trailing edge of tail fin. It implies that the vortex structure in wake behind the fish is related to the mechanism of propulsive forces. The blade element theory which is originally used to determine the behavior of propeller is applied to study the thrust of flapping pectoral fins. The forces are obtained by integrating along the entire blade based on a steady solution. However, the theory becomes unwieldy if the number of elements or large time intervals must be small.

In spite of the above important works, several questions remain unanswered satisfactorily. It is widely known that fish swim at high but finite Reynolds number flow where inertial forces dominate. Nevertheless, viscous effects are responsible for vorticity generation and therefore a force theory based on the real viscous flow is amenable to full flow analysis. Next, as a fish accelerates to swim forward, we have the equation of motion ma = T-D according to Newton's Second Law. Obviously, thrust T and drag D exerted on the body are along the same line at the same time. Generally speaking, there was no comprehensive theory that had been applied to distinguish whether a flow element contribute to drag or to thrust (except the potential forces). Recently, Lauder (2011) reviewed swimming hydrodynamics and proposed ten questions needed to resolve. He remarked in his article "Although quite a few papers have investigated the effects of flexibility on aquatic locomotor performance (e.g., Alben *et al*., 2004; Alben, 2008; Shoele and Zhu, 2009), we still lack basic information on how flexible natural biologic systems are and hence on how much changes in flexibility affect locomotor parameters such as thrust generation and efficiency." Besides, some theories are presented to explain the mechanisms of the thrust for specific fish but are not applicable to explain others. For instant, Elongated body theory (Lighthill, 1960) is suitable to analyze Anguilliform swimming of BCF modes whilst failing to predict thrust for Tunalliform swimming of BCF, which has to resort to the foil theory (Wagner *et al*., 1925). This shows that it still lacks a unified theory to explain the mechanisms of flexible effects for the diversity of motions of organisms.

MATERIALS AND METHODS

In this study, the unsteady thrust mechanisms of the flexible motion are investigated from the viewpoint of the force decomposition theory (Howe, 1976, 1989, 1991, 1995). The force decomposition theory is usually used to separate potential forces and to distinguish the contributions of individual fluid elements to aerodynamic forces in real flow. It starts from D'Alembert theorem that incompressible potential flow predicts that no force will be exerted on a body if the incident flow is a constant uniform stream. Incompressible potential flow means that there is no single fluid element possessing non-zero vorticity or dilation. In addition, the force decomposition theory was extended to study the problem of the high lift generation of the insect flights (Lee *et al*., 2012; Hsieh *et al*., 2010, 2009). On the other hand, the early idea that forces experienced by the body in terms of the vorticity distribution which is similar to this present study, was reviewed by Biesheuvel and Hagmeijer (2006). They pointed out the close relationship of Burgers' formula to those by Lighthill (1969, 1986). These researchers went further to establish the connection between these earlier formulas and the more recent work

on the aerodynamic forces by Kambe (1986) and Howe *et al.* (2001). Finally, we note a recent paper by Magnaudet (2011) which provides a general form for the prediction of loads on a body moving in an arbitrary non-uniform flow.

In present study, the thrust mechanisms of the flexible motion are investigated. The model is the deforming body by creating an advancing wave from its leading edge to trailing edge which demonstrates the motion of all length of a fish with low aspect ratio fin.

Auxiliary potential: In order to analyses various force contributions to the flow over a self-deformation body, we need to introduce auxiliary potential functions. Let us first determine the nature of potential solution. The potential solution φ satisfies $\nabla\varphi^2 = 0$ and is required to vanish at infinity. The general solution at great distances r from the deformable body in two dimensions is given by:

$$\varphi = -(A\cdot\nabla)\log r + \cdots = -\frac{A\cdot\hat{r}}{r} + \cdots \quad (1)$$

where, r is the unit vector along the direction of r. In Eq. 1 the vector depends on the actual shape and the motion of the flexible body and is independent of the coordinates. The exact A requires a complete solution of the equation $\nabla\varphi^2 = 0$ and appropriate boundary conditions. It should be kept in mind that the corresponding velocity $\nabla\varphi$ decay like $1/r^2$ in two dimensions. The boundary conditions will be specified depending on which force direction is considered. If s is the unit vector along the force direction of interest, then we require n. $\nabla\varphi$ = -ns on the body surface. The potential function that satisfies this condition is used to decompose the pressure force along the s-direction for real viscous fluid to added-mass force, surface vorticity force, volume vorticity force as well as other possible contributions.

The force decomposition: Consider a deformable body motion in water as shown in Fig. 1. Let p be the water density, μ the water viscosity, L the chord length, U is the inflow velocity. Take L to be the reference length, L/U to be the reference time and pLU^2 to be the reference pressure. The flow field of the deforming motion is assumed to be governed by the Navier-Stokes equations and incompressibility condition which, in dimensionless form are given by:

$$\frac{\partial v}{\partial t} + (v\cdot\nabla)v = -\nabla p + \frac{1}{Re}\Delta v \quad (2)$$

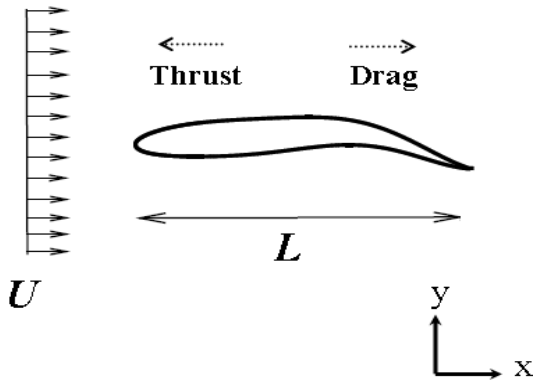

Fig. 1: Schematic of flow about a deformable body where is the inflow velocity and is the chord length. The force excerted on the body of which direction same as the inflow direction is drag but opposite is thrust

$$\nabla\cdot v = 0 \quad (3)$$

Where:

p = The pressure

v = The velocity and Re=pLU

μ = The Reynolds number. The most well-known formula for calculating the drag is

$$C_D = \underbrace{\int_S pn\cdot i dA}_{C_{Dp}} + \underbrace{\frac{1}{Re}\int_S n\times\omega\cdot i dA}_{C_{Df}} \quad (4)$$

Where:

I = The unit vector in the drag direction

n = The inward normal to the wing surface and

ω = Denotes the vorticity

Now we show how to gain the formula of force decomposition. First of all, we are concerned with the drag direction. Let φ satisfy the boundary condition n. $\nabla\varphi$ = -n. I (i.e.,) s = i) which means the unit velocity on the body. Let V_R be the volume of fluid enclosed by a circle surface S_R of large radius and the body surface S. Equation 2 can be written:

$$-\nabla p = \frac{\partial v}{\partial t} + \frac{1}{2}\nabla|v|^2 - v\times\omega + \frac{1}{Re}\nabla\times\omega \quad (5)$$

Here, we will use the two identities $v.\nabla\varphi = \nabla.(v\varphi)$ and $(\nabla\times\omega)$. $\nabla\varphi = \nabla.(\omega\times\nabla\varphi)$ and apply the divergence theorem. Taking inner products with on both sides of Eq. 5 and integrating within the flow region V_R yields:

$$-\int_{S\cup S_R} pn\cdot\nabla\varphi dA=\int_{S\cup S_R}\varphi\frac{\partial v}{\partial t}\cdot ndA+\frac{1}{2}\int_{S\cup S_R}|v|^2\nabla\varphi\cdot ndA-\int_{V_R} v\times\omega\cdot\nabla\varphi dV+\frac{1}{Re}\int_{S\cup S_R} n\times\omega\cdot\nabla\varphi dA \quad (6)$$

The fluid is non-vorticity in the far field from the body. Applying this boundary condition and noting that $\nabla\varphi$ decays like $1/r^2$, we can carry out the integral on the left-hand side and the first, second and fourth ones on the right hand side with $R\to\infty$ and $V_R\to V$ (entire fluid region). Besides, recall the boundary condition n the. $\nabla\varphi$ = -n.i on the body surface for the left hand side to obtain:

$$\underbrace{\int_S pn\cdot idA}_{C_{Dp}}=\underbrace{\int_S\varphi\frac{\partial v}{\partial t}\cdot ndA}_{C_{Da}}+\underbrace{\frac{1}{2}\int_S|v|^2\nabla\varphi\cdot ndA}_{C_{Dm}}\underbrace{-\int_V v\times\omega\cdot\nabla\varphi dV+\frac{1}{Re}\int_S n\times\omega\cdot\nabla\varphi dA}_{C_{Dv'}} \quad (7)$$

If the frictional forc $C_{Df}=1/Re\int_s n\times\omega$ idA on the right hand side of Eq. 4 is included and combine it with the surface integral vorticity force $1/Re\int_s n\times\omega$ $\nabla\varphi$dA of the third term in Eq. 7 the complete decomposition for the drag force can be obtained:

$$C_D=\underbrace{\int_S\varphi\frac{\partial v}{\partial t}\cdot ndA}_{C_{Da}}+\underbrace{\frac{1}{2}\int_S|v|^2\nabla\varphi\cdot ndA}_{C_{Dm}}\underbrace{-\int_V v\times\omega\cdot\nabla\varphi dV}_{C_{Dv}}+\underbrace{\frac{1}{Re}\int_S n\times\omega\cdot\nabla\varphi dA}_{C_{Ds}} \quad (8)$$

In Eq. 7 and 8 C_{da} is the contribution associated with the added-mass force of the deforming body, C_{dm} corresponds to the contribution by the velocity of the wing, C_{Ds} denotes the contribution by the surface vorticity and friction on the body surface and C_{Dv} represents the contribution of pressure force due to vorticity within the flow field. In particular, the integrand-$v\times\omega$. $\nabla\varphi$ is called the volume drag element and 1/Re $n\times\omega$. ($\nabla\varphi$+j) is called the surface drag element where the part with $\nabla\varphi$ is called the friction-like force. Either of them may be termed the vortex force elements. A salient feature is: only the volume drag elements near the body contribute significantly to the drag force because $\nabla\varphi$ is rapidly decaying away from the body. Also, the potential function φ can be considered as the geometric factor for each flow condition can be associated with a unique φ. It is noted that among the force components, C_{da} and C_{Dm} are determined by the boundary conditions and the geometric profile while the determination of C_{Dv} and C_{Ds} requires solution of the fluid flow. Note that if we consider the force in lift direction, say s = J, then φ has to satisfy n. $\nabla\varphi$ = -n. J on the flexible body surface. The force along the j-direction is decomposed by:

$$C_L=\underbrace{\int_S pn\cdot jdA}_{C_{Lp}}+\underbrace{\frac{1}{Re}\int_S n\times\omega\cdot jdA}_{C_{Lf}}=\underbrace{\int_S\varphi\frac{\partial v}{\partial t}\cdot ndA}_{C_{La}}+\underbrace{\frac{1}{2}\int_S|v|^2\nabla\varphi\cdot ndA}_{C_{Lm}}\underbrace{-\int_V v\times\omega\cdot\nabla\varphi dV}_{C_{Lv}}+\underbrace{\frac{1}{Re}\int_S n\times\omega\cdot(\nabla\varphi+j)dA}_{C_{Ls}} \quad (9)$$

Here, the numerical results are obtained by the SIMPLEC method of the commercial code Ansys FLUENT based on the control-volume method. Moreover, a conformal-hybrid grid is used in the numerical method. In each time interval, the grid deformation is adjusted by the deformation of the body to achieve numerical stability, according to the method of spring analogy and remeshing, and governed by the Geometric Conservation Law (GCL) (Thomas and Lombard, 1979). In the present study, the total drag coefficient C_D is obtained by summing up all the drag components, C_{Dm}, C_{da}, C_{dv} and C_{Ds}. To ensure its accuracy, C_D will also be computed according to Eq. 4 and the computed result is denoted by C_D (p).

RESULTS ND DISCUSSION

The present force representation will be applied to the fish-like undulation motion and heaving motion with particular emphasis on the individual effects of the thrust and drag elements. Here, we consider a uniform flow passing through a deformable body with NACA0012 in shape. To compare the mechanisms of the two motions consistently, the Reynolds number Re = LU/v is fixed at 5000 in this study.

The motions of undulating model are be concerned. The lateral deformation y_m of the undulating body is according to Y (x, y) = A (x) cos ($2\pi L/\lambda$(x-ct)) where A (x) is the amplitude with variation with the each body element position, c is the progressing wave speed and λ is the wavelength of the wave. Based on investigation of the kinematic data of steadily swimming saith (Videler, 1993), the amplitude of the body wave can be described by $A(x)=A_0+A_1x+A_2x^2$ and the coefficients A_0, A_1 and A_2 are solved by A (0) = 0.02, A (0.2) = 0.01 and

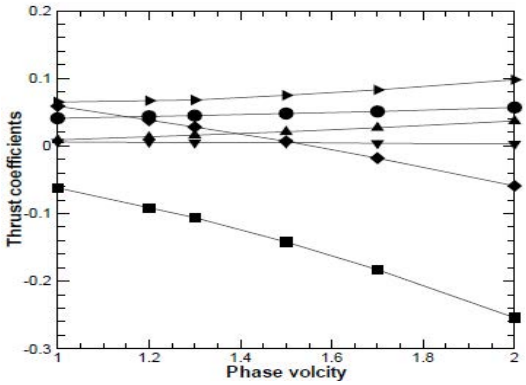

Fig. 2: Averaged drag coefficients versus the phase speed (C_{Dv}, C_{Df}, C_{Dm} , C_{Ds}, C_D, C_{Da}). It has to been noted that the negative means the thrust generation

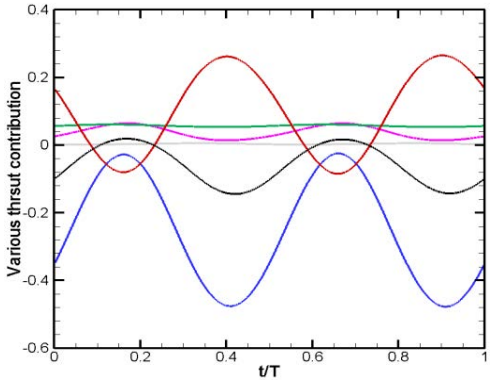

Fig. 3: Time histories of the drag contribution for the phase speed c = 2.0 (Bleak: C_D; Purple: C_{Dm}; Blue: C_{Da}; Green: C_{Df}; Red: C_{Df}; Gray: C_{Ds})

A (1) = 0.10. Another significant non-dimension parameter that characterize hydrodynamic performance for the fish undulation is Strouhal number which is defined as St = fA/U where f is beat frequency of a fish.

To start with the discussion, the various thrust contributions for the undulations as a function of phase speed c in the range from 1.0-2.0, corresponding to Strouhal number St within the interval 0.2-0.4 which lies in the regime of swimming animals, under the condition of assuming the constant uniform free-stream velocity and the peak-to-peak amplitude were analyzed. This motion physical parameter setting could lead us to understand the propulsive mechanisms of live fish in nature. (Fig. 1).

Figure 2 shows the average total drag force C as well as the five thrust components, C_{Dm}, C_{Da}, C_{df} , C_{Dv} and C_{ds} versus the phase speed c. The average drag chas the maximum (= 0.06, drag force) at c = 1.0, decreasing to nearly zero in a range near c = 1.05 and to the minimum (= -0.06, thrust force) at c = 2.0 where an undulating foil gains a net thrust force to swim forward in a uniform flow. This behavior of the can be analyzed by explaining the various contributions of the constituent force components. The drag C_{ds} is uniformly small and negligible compared to other components for all c. By increasing the phase speed, the C_{Df} and C_{Dm} increase slightly and the relative ratios of increasing from c = 1.0 to 2.0 are 0.02 and 0.03, respectively. As far as volume-vorticity contribution C_{Dv} is concerned, the value acts as drag force and becomes larger with increasing c. Also, the increasing ratio of C_{dv} from c = 1.0-2.0 is 0.04 which implies that an undulating foil gains larger drag force from the vorticity in the flow field with the increase in phase speed.

However, a flexible foil gaining a propulsive force -C_D is completely credited to the added-mass force C_{Da} which is negative and significantly decreases with increasing c. The increasing ratio of C_{Da} for the case c = 2.0 compared to c = 1.0 is 0.2 which is not only enough to overcome other increasing of drag contributions, C_{dm}, C_{df} and C_{Dv} due to increasing in c but also provides extra propulsive contribution to total thrust C_D. Meanwhile, we note that the drag contribution from the pressure term (C_{dp} = C_{dm}+C_{Da}+C_{Ds}+C_{Dv}) is close to zero for a cruise swimming motion in the case of phase speed. It is consistent with Wu's theoretical prediction based on the inviscid flow analysis (only consider the pressure force and neglects the viscous force).

In order to elucidate the unsteadiness, Fig. 3 shows the time histories of the total drag C_D as well as the five thrust components C_{Dm}, C_{Da}, C_{Df}, C_{Dv} and C_{Ds} for the phase c = 2 in a period of undulation after reaching a periodic state. In the beginning of the period, the tail of the foil is located at a maximum 0.1 in a lateral direction where the phase velocity is just equal to zero. First, we observe one maximum and one minimum in the total drag C_D as well as in the added-mass, volume-vorticity, velocity components, C_{Da}, C_{dv} and C_{Dm} in a half undulating period (t/T = 0-0.5). Besides, the behaviors of, C_D, C_{dm} and C_{Da} are similar, while that of C_{Dv} is inverse to them. More detail, we note that C_{Ds} is uniformly small and can be neglected. For friction force, C_{df} it is uniformly positive (0.4) in a full period. The time history curve for C_{Dm} is also entirely positive. Consider, C_{dv}, it is obvious that C_{Dv} is positive most of the time and the maximum (= 0.26) occurs when t/T = 0.4. However, an interesting point is minimum C_{Dv} (-0.48, thrust) appearing in the stage in which the tail of the undulating foil accelerate closely to the maximum. We will explain this according to the volume-drag element

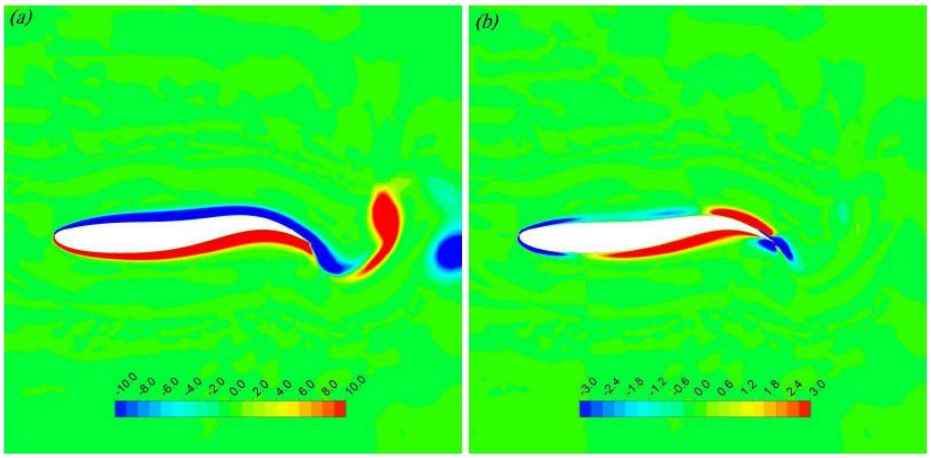

Fig. 4: Maximun thrust for the case c = 2.0 at t/T = 0.16: a) vorticity contour (red, anticlockwise; blue, clockwise) and b) thrust force element contour (red, drag elements; blue, thrust element)

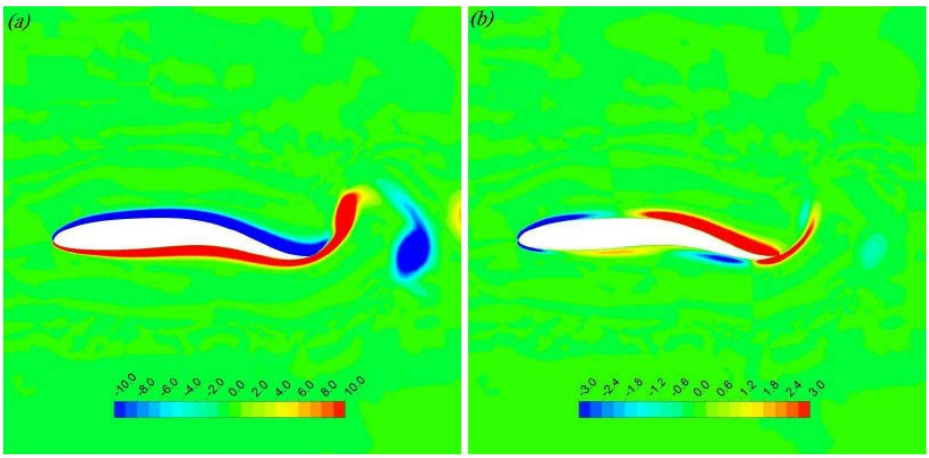

Fig. 5: Maximun drag for case c = 2.0 at t/T = 0.41: a) at (a) vorticity contour (red, anticlockwise; blue, clockwise) and b) thrust force element contour (red, drag elements; blue, thrust element)

contour later. Turn to investigate the added-mass force contribution. C_{Da} is negative all of the time which means that an undulating mainly maintains a positive total thrust $-C_D$ because of the positive contributions-C_{Da}. More detail, the minimum (= -0.48) occurs when t/T = 0.41 while the maximum C_{Da} (= -0.03) occurs when t/T = 0.16. In summary, the instantaneous thrust $-C_D$ required for the propulsive motion of the foil consists of added-mass and volume-vorticity forces. In particular, the conditions for maintaining the positive $-C_D$ are added-mass force attains the maximum to balance the drag generated by volume-vorticity forces. As added mass forces decreases to the minimum, the volume-vorticity force could immediately provide some positive contribution to the total thrust to offset. It could be concluded that an undulating foil smoothly operates and appropriately modulates added-mass and volume-vorticity forces to gains force to swim forward.

Here, we choose the case of phase speed c = 2 to examine how to gain instantaneous thrust force from vorticity in the surrounding flow generated by an undulating motion. These behaviors can be examined closely by exploring the distributions of volume vortex elements at different times. Before we proceed with the details, we emphasize that a region of vorticity of the same sigh may contribute both positive and negative. Whether we have net positive or net negative force elements depends on the instant shape of the fish foil and the actual flow condition. Figure 4 and 5 show two snapshots of vorticity and volume-thrust elements when n

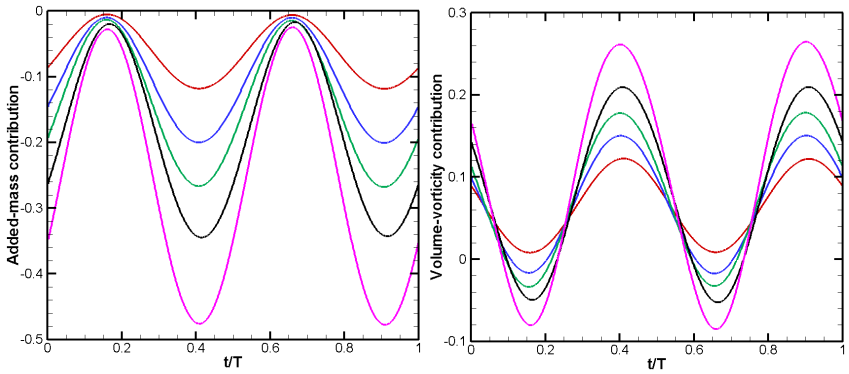

Fig. 6: Time history of the added-mass and volume-vorticity contribution for the different phase speed

undulating foil obtains the maximum thrust (= 0.02) and drag (= 0.14) at t/T = 0.16 and t/T = 0.41, respectively. In Fig. 4 and 5, it is found that the strong shear layers of different sighs are generated along the undulating foil surface. These strong shear layers gradually shed into down stroke to form a reverse von Karman vortex-street. It has been concluded that this vortex structure induces a jet mean velocity profile in the wake and leads to the generation of the thrust. However, it is not totally enough to explain high thrust mechanism of an undulating foil from our perspective. Figure 4b shows that the vortex layers round the leading edge of the foil provides large thrust elements (Red). Also, an important mechanism we found is that the slender vorticity located at a wind side of the foil provides drag forces while that located at a leeside of the foil provides thrust forces. Interestingly, these slender drag and thrust elements are followed by the motion of the body travelling wave to the tail. As the thrust elements (blue) just shed into the wake and are enhanced by the acceleration of the tail, C_{dv} will attain to the minimum (Fig. 4b). Similarly, attains to the maximum while the slender drag elements shed into the wake, showed in Fig. 5b. Next, we pay attention on the time-independent $C_{da\ Dv}$ and during one circle for different phase speeds in Fig. 6. It is shown that two local maximum and minimum are identified during one period. It is found that as c increases, C_{da} and C_{Dv} varies largely. Besides, C_{da} is negative for all phase speed c. For C_{Dv}, it could be negative during some time intervals in a cycle for c>1.0, except the case of c = 1.0 (C_{dv} is all positive).

CONCLUSION

Using the force decomposition theory, the mechanisms of thrust and drag generated by the two-dimension representation of an undulation swimming motion was investigated in this study. The unsteadiness effects of the undulation propulsion includes the added-mass produced by the body acceleration and the vorticity within in flow field and that on the body surface. In the results, it is clear that added-mass force is the most significant thrust source among all considered motions and arrangements. Also, the vortices round the leeside of deformable body are beneficial for thrust generation is found by identifying the variations of the vorticity thrust elements with various flow structures. However, the average volume vorticity contribution is opposite to bionic structure forward. All in all, the results of this study the theory proposed by Lighthill and Wu and have same conclusion to explain propulsion of fish. On the other hand, the phenomenon of the oscillatory motion of the bionic structure is also an interesting work in the future work.

ACKNOWLEDGEMENT

This research is supported by the Ministry of Science and Technology under Grant No. MOST 104-2221-E-165-002, Taiwan.

REFERENCES

Alben, S., 2008. Optimal flexibility of a flapping appendage in an inviscid fluid. J. Fluid Mech., 614: 355-380.

Alben, S., M. Shelley and J. Zhang, 2004. How flexibility induces streamlining in a two-dimensional flow. Phys. Fluids, 16: 1694-1713.

Biesheuvel, A. and R. Hagmeijer, 2006. On the force on a body moving in a fluid. Fluid Dyn. Res., 38: 716-742.

Blake, R.W., 1983. Energetics of leaping in dolphins and other aquatic animals. J. Mar. Biol. Assoc. UK., 63: 61-70.

Howe, M.S., 1976. Contributions to the theory of aerodynamic sound, with application to excess jet noise and the theory of the flute. J. Fluid Mech., 71: 625-673.

Howe, M.S., 1989. On unsteady surface forces and sound produced by the normal chopping of a rectilinear vortex. J. Fluid Mech., 206: 131-153.

Howe, M.S., 1991. On the estimation of sound produced by complex fluid-structure interactions, with application to a vortex interacting with a shrouded rotor. Proceedings of the Royal Society of London A: Mathematical, Physical and Engineering Sciences, June 1-8, 1991, The Royal Society, London, England, pp: 573-598.

Howe, M.S., 1995. On the force and moment on a body in an incompressible fluid, with application to rigid bodies and bubbles at high and low Reynolds numbers. Q. J. Mech. Appl. Math., 48: 401-426.

Howe, M.S., G.C. Lauchle and J. Wang, 2001. Aerodynamic lift and drag fluctuations of a sphere. J. Fluid Mech., 436: 41-57.

Hsieh, C.T., C.C. Chang and C.C. Chu, 2009. Revisiting the aerodynamics of hovering flight using simple models. J. Fluid Mech., 623: 121-148.

Hsieh, C.T., C.F. Kung, C.C. Chang and C.C. Chu, 2010. Unsteady aerodynamics of dragonfly using a simple wing-wing model from the perspective of a force decomposition. J. Fluid Mech., 663: 233-252.

Kambe, T., 1986. Acoustic emissions by vortex motions. J. Fluid Mech., 173: 643-666.

Lauder, G.V., 2011. Swimming hydrodynamics: Ten questions and the technical approaches needed to resolve them. Experiments Fluids, 51: 23-35.

Lee, J.J., C.T. Hsieh, C.C. Chang and C.C. Chu, 2012. Vorticity forces on an impulsively started finite plate. J. Fluid Mech., 694: 464-492.

Lighthill, J., 1986. Fundamentals concerning wave loading on offshore structures. J. Fluid Mech., 173: 667-681.

Lighthill, M.J., 1960. Note on the swimming of slender fish. J. Fluid Mech., 9: 305-317.

Lighthill, M.J., 1969. Dynamic response of the Indian Ocean to onset of the southwest monsoon. Philosophical Trans. Royal Soc. London Math. Phys. Eng. Sci., 265: 45-92.

Lighthill, M.J., 1970. Aquatic animal propulsion of high hydromechanical efficiency. J. Fluid Mech., 44: 265-301.

Magnaudet, J., 2011. A reciprocal theorem for the prediction of loads on a body moving in an inhomogeneous flow at arbitrary Reynolds number. J. Fluid Mech., 689: 564-604.

Sfakiotakis, M., D.M. Lane, J.B.C. Davies, 1999. Review of fish swimming modes for aquatic locomotion. IEEE J. Oceanic Eng., 24: 237-252.

Shoele, K. and Q. Zhu, 2009. Fluid-structure interactions of skeleton-reinforced fins: Performance analysis of a paired fin in lift-based propulsion. J. Exp. Biol., 212: 2679-2690.

Thomas, P.D. and C.K. Lombard, 1979. Geometric conservation law and its application to flow computations on moving grids. AIAA J., 17: 1030-1037.

Videler, J.J., 1993. Fish Swimming. Vol. 10, Springer Science & Business Media, Berlin, Germany,.

Wagner, E., K.F. Meyer and C.C. Dozier, 1925. Studies on the metabolism of B Botulinus in various media. J. Bacteriol., 10: 321-412.

Wu, J.C., 1981. Theory for aerodynamic force and moment in viscous flows. AIAA. J., 19: 432-441.